

Transient simulation temperature field for continuous casting steel billet and slab

Josef Stetina, Frantisek Kavicka, Tomas Mauder, Lubomir Klimes

Brno University of Technology, Technicka 2, Brno, Czech Republic, +420541143269, stetina@fme.vutbr.cz

The presented models are valuable computational tools and accurate simulators for investigating transient phenomena in billet and slab caster operations, and for developing control methods, the choice of an optimum cooling strategy to meet all quality requirements, and an assessment of the heat-energy content required for direct rolling. The numerical models of temperature field in the continuous casting are determined via the transient 3D enthalpy balance equation with the Finite Differences Method.

The transient simulation is undergoing a non-stop trial run in one operation because steel billets/slabs are produced 24 hours per day. The numerical computation has to take place simultaneously with the data acquisition – not only to confront it with the actual numerical model, but also to make it more accurate throughout the process. It enables a multiple increase in the speed with which the temperature field of the continuous casting is computed – both with the application of more sophisticated software as well as hardware. As a result of this, it will be possible to monitor the formation of the temperature field – in real time – within the mould, the secondary- and maybe even the tertiary-cooling zones, and also to utilize this information for the optimization of the control of the caster as a whole as well as its individual parts.

There are examples of the application of the models on the temperature field of a real concast billet and slab on Trinecke zelezarny and Evraz Vitkovice Steel.

Key words: temperature field, solidification, simulation, billet, slab

Introduction

The production of steels, alloys and metallurgical products in general is constantly developing. Materials with high utility parameters are more in demand and traditional production is being replaced by higher quality steel. More and more sophisticated aggregates using more sophisticated technological procedures are being implemented. In order to maintain competitiveness, diversify the production and expand to other markets, it is necessary to monitor the technological development. In the case of concasting, it is not possible to fulfill these requirements without the application of models of all caster processes dependent on thermal-mechanical relationships. These models can be applied both off-line and on-line. An off-line model is one where the calculation takes longer than the time of the actual casting process. An on-line model runs in real time – taking the data directly from the operation – and its calculation takes the same time (if not less) than the actual process.

These models will support the design of new and redesign of old machines, they will facilitate the identification and quantification of any potential defects and optimization of the various operational conditions in order to increase the productivity and minimize (the occurrence) defects. The process of the solidification of concast steel is influenced by many factors and conditions, among which are the following:

- Complete turbulent transient flow within a comprehensive geometry (input jet and liquid metal in the slab)

- Thermodynamic reactions between the casting powder and the solidifying slab
- Heat transfer between the liquid and solid powder on the surface of the slab
- Dynamic movement of the liquid steel inside the mould on the liquid phase-mushy zone interface, including the influence of gravity, oscillations and the casting speed
- Heat transfer in a superheated melt considering turbulent flow
- Transition (mixture) composition of the steel during the change of class
- Heat and mechanical interaction in the area of the meniscus between the solidifying meniscus, the solid powder and liquid steel
- Heat transfer from the surface of the solidified shell into the space between the shell and the working surface of the mould (including the layers of the casting powder and the air gap)
- Mass transfer of the powder during its vertical movement through the gap between the shell and the mould
- Contact of the solidified slab with the mould and support rollers
- The occurrence of crystals inside the melt
- The process of micro-segregation and macro-segregation
- The occurrence of shrinkages as a result of temperature contraction of the steel and the initialization of internal stress
- The occurrence of stress and strain in the solidified shell as a result of external influences such as friction

inside the mould, bulging between rollers, rolling, temperature stress and strain

- The occurrence of cracks as a result of internal stress
- The flow of steel as a result of electromagnetic stirring and the influence of the stirring on the temperature field and the primary structure
- The occurrence of stress and strain as a result of unbending of the inside of the segments or in the rolling mill
- Radiation between the various surfaces
- Cooling as a result of convection beneath the water or water-air jets

With respect to the complexity of the investigation into the influences of all above-mentioned factors, it is not possible to develop a mathematical model that would cover all of them. It is best to group them according to the three main types of influences:

- Heat and mass transfer
- Mechanical
- Structural

The primary and deciding one is the influence of heat and mass transfer because it is the temperature field that gives a rise to mechanical and structural influences. The development of a model of the temperature field (of a slab) with an interface for providing data for mechanical stress and strain models and structure models is therefore a top-priority task [1].

A model of the temperature field of a blank

The presented in-house model of the transient temperature field of the blank from a billet caster (Figure 1) is unique in that, in addition to being entirely 3D, it can work in real time. It is possible to adapt its universal code and implement it on any billet caster. The numerical model covers the temperature field of the complete length of the blank (i.e. from the meniscus inside the mould all the way down to the cutting torch) with up to one million nodes.

The solidification and cooling of a blank and the simultaneous heating of the mould is a case of 3D transient heat and mass transfer in a system comprising the blank-mould-ambient and, after leaving the mould, it is a system comprising only the blank-ambient. If mass transfer is neglected and if only conduction is considered as decisive, then the heating up of the mould is described by the Fourier equation (1) and the solidification and cooling of the blank is described by the Fourier-Kirchhoff equation (2), which contains the components describing the heat flow from the melt flowing with a velocity v and the component including the internal source of latent heats of phase or structural changes.

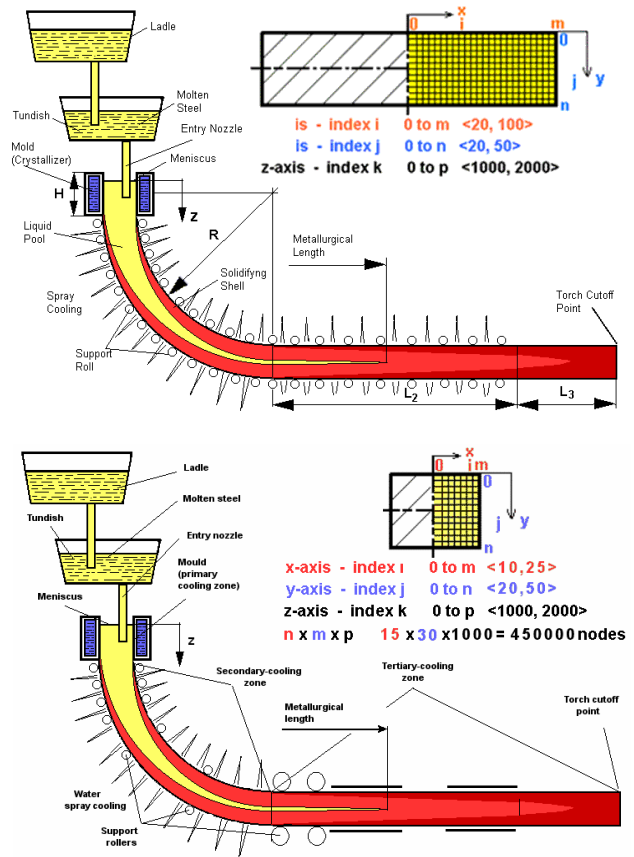


Figure 1: Slab and billet caster

$$\rho \cdot c \frac{\partial T}{\partial \tau} = \frac{\partial}{\partial x} \left(k \frac{\partial T}{\partial x} \right) + \frac{\partial}{\partial y} \left(k \frac{\partial T}{\partial y} \right) + \frac{\partial}{\partial z} \left(k \frac{\partial T}{\partial z} \right) \quad (1)$$

$$\rho \cdot c \frac{\partial T}{\partial \tau} = \frac{\partial}{\partial x} \left(k \frac{\partial T}{\partial x} \right) + \frac{\partial}{\partial y} \left(k \frac{\partial T}{\partial y} \right) + \frac{\partial}{\partial z} \left(k \frac{\partial T}{\partial z} \right) + \rho \cdot c \left(v_x \frac{\partial T}{\partial x} + v_y \frac{\partial T}{\partial y} + v_z \frac{\partial T}{\partial z} \right) + \dot{Q}_{source} \quad (2)$$

Figure 2 shows the temperature balance of an elementary volume representing a general node of the mesh (i,j,k) inside the mould. The heat conductivities VX , VY and VZ along the main axes are:

$$VX_{i,j,k} = k_i \frac{A_x}{\Delta x} \quad VX_{i-1,j,k} = k_{i-1} \frac{A_x}{\Delta x} \quad (3a)$$

$$VY_{i,j,k} = k_j \frac{A_y}{\Delta y} \quad VY_{i,j-1,k} = k_{j-1} \frac{A_y}{\Delta y} \quad (3b)$$

$$VZ_{i,j,k} = k_k \frac{A_z}{\Delta z} \quad VZ_{i,j,k-1} = k_{k-1} \frac{A_z}{\Delta z} \quad (3c)$$

The heat flows QX, QY and QZ through the elementary volume along the main axes are:

$$QX = VX_{i,j,k} (T_{i+1,j,k}^{(\tau)} - T_{i,j,k}^{(\tau)}) \quad (4a)$$

$$QX1 = VX_{i-1,j,k} (T_{i-1,j,k}^{(\tau)} - T_{i,j,k}^{(\tau)}) \quad (4b)$$

$$QY_i = VY_{i,j,k} (T_{i,j+1,k}^{(\tau)} - T_{i,j,k}^{(\tau)}) \quad (4c)$$

$$QY1_i = VY_{i,j-1,k} (T_{i,j-1,k}^{(\tau)} - T_{i,j,k}^{(\tau)}) \quad (4d)$$

$$QZ_{i,j} = VZ_{i,j,k} (T_{i,j,k+1}^{(\tau)} - T_{i,j,k}^{(\tau)}) \quad (4e)$$

$$QZ1_{i,j} = VZ_{i,j,k-1} (T_{i,j,k-1}^{(\tau)} - T_{i,j,k}^{(\tau)}) \quad (4f)$$

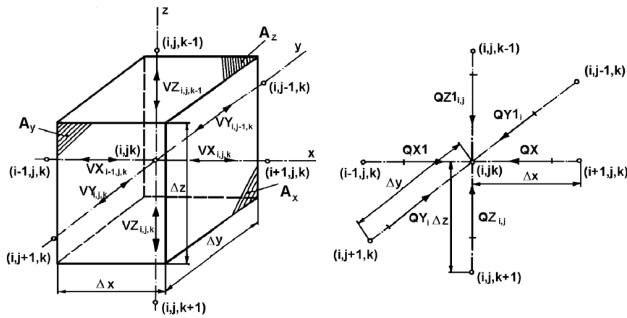


Figure 2: Heat balance of a general node of the mesh

The temperature balance of the general node is:

$$(QZ1_{i,j} + QZ_{i,j} + QY1_i + QY_i + QX1 + QX) = \frac{\Delta x \cdot \Delta y \cdot \Delta z \cdot \rho \cdot c}{\Delta \tau} (T_{i,j,k}^{(\tau+\Delta \tau)} - T_{i,j,k}^{(\tau)}) \quad (5)$$

where the right hand side expresses the accumulation (or the loss) of heat in the node (i,j,k) during the time step Δτ. The unknown temperature of the general node of the mesh inside the mould in the following instant (τ+Δτ) is therefore given by the explicit formula:

$$T_{i,j,k}^{(\tau+\Delta \tau)} = T_{i,j,k}^{(\tau)} + \frac{(QZ1_{i,j} + QZ_{i,j} + QY1_i + QY_i + QX1 + QX) \cdot \Delta \tau}{\Delta x \cdot \Delta y \cdot \Delta z \cdot \rho \cdot c} \quad (6)$$

The temperature field of the blank passing through a radial caster of a large radius can be simplified by the Fourier-Kirchhoff equation where only the v_z component of the velocity is considered. Equation (2) is therefore reduced to:

$$\rho \cdot c \frac{\partial T}{\partial \tau} = \frac{\partial}{\partial x} \left(k \frac{\partial T}{\partial x} \right) + \frac{\partial}{\partial y} \left(k \frac{\partial T}{\partial y} \right) + \frac{\partial}{\partial z} \left(k \frac{\partial T}{\partial z} \right) + \rho \cdot c \cdot v_z \frac{\partial T}{\partial z} + \dot{Q}_{source} \quad (7)$$

Equation (7) must cover the temperature field of the blank in all three stages: above the liquidus temperature (i.e. the melt), in the interval between the liquidus and solidus temperatures (i.e. the so-called mushy zone) and beneath the solidus temperature (i.e. the solid phase). It is therefore convenient to introduce the thermodynamic function of specific volume enthalpy $H_v = c \cdot \rho \cdot T$, which is dependent on temperature, and also includes the phase and structural heats (Figure 3).

Heat conductivity k , specific heat capacity c and density ρ are thermophysical properties that are also functions of temperature. Equation (7) therefore takes the form:

$$\frac{\partial H_v}{\partial \tau} = \frac{\partial}{\partial x} \left(k \frac{\partial T}{\partial x} \right) + \frac{\partial}{\partial y} \left(k \frac{\partial T}{\partial y} \right) + \frac{\partial}{\partial z} \left(k \frac{\partial T}{\partial z} \right) + v_z \frac{\partial H_v}{\partial z} \quad (8)$$

The heat balance of the elementary node is:

$$(QZ1_{i,j} + QZ_{i,j} + QY1_i + QY_i + QX1 + QX) = \frac{\Delta x \cdot \Delta y \cdot \Delta z}{\Delta \tau} (H_{v,i,j,k}^{(\tau+\Delta \tau)} - H_{v,i,j,k}^{(\tau)}) \quad (9)$$

where the heat flow QZ_{i,j} now must also include the enthalpy of the incoming volume of melt:

$$QZ_{i,j} = VZ_{i,j,k} (T_{i,j,k+1}^{(\tau)} - T_{i,j,k}^{(\tau)}) - A_z \cdot v_z \cdot H_{v,i,j,k}^{(\tau)} \quad (10)$$

The unknown enthalpy of the general node of the blank in the following instant ($\tau+\Delta\tau$) is given by the explicit formula, similar to Equation (6):

$$H_{v,i,j,k}^{(\tau+\Delta\tau)} = H_{v,i,j,k}^{(\tau)} + (QZ_{1,i,j} + QZ_{2,i,j} + QY_{1,i} + QY_{2,i} + QX_{1,i} + QX_{2,i}) \frac{\Delta\tau}{\Delta x \cdot \Delta y \cdot \Delta z}$$



Figure 3: The enthalpy function for steel showing the phase and structural changes

Figure 3 indicates how the temperature model for the calculated enthalpy in Equation (11) determines the unknown temperature.

The next task is to choose a suitable coordinate system and mesh. This paper deals with the symmetrical half of one cross-section of a blank from the meniscus inside the mould down to the cutting torch. The origin of the coordinate system is positioned on the small radius in the centre of the width (Figure 4). This enables all coordinates to be positive, which facilitates software programming. In the region of the radius, the Cartesian coordinates are transformed into cylindrical (i.e. y is the radius and z is the angle). The mesh is generated automatically and the model supports all densities of the mesh introduced in Figure 4. All results presented in this paper are based on a mesh of 573,594 nodes (11 in the x -direction, 21 in the y -direction and 1861 in the z -direction) and a $7.5 \times 7.5 \times 15$ mm elementary volume.

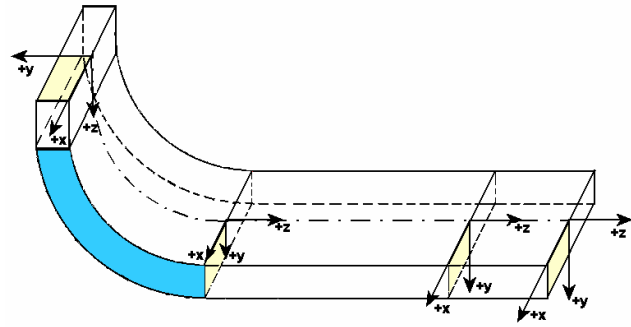


Figure 4: The mesh and definition of the coordinate system

All thermodynamic properties of the cast steel, dependent on its chemical composition and cooling rate, enter the calculation as functions of temperature [2]. This is therefore a significantly non-linear task because, even with the boundary conditions, their dependence on the surface temperature of the blank is respected here.

Regarding the fact that the task can be considered symmetrical along the axis (Figure 4), it is sufficient to deal with only one half of the cross-section. The boundary conditions are therefore as follows:

$$1. \quad T = T_{cast} \quad \text{the level of the steel} \quad (12a)$$

$$2. \quad -k \frac{\partial T}{\partial n} = 0 \quad \text{the plane of symmetry} \quad (12b)$$

$$3. \quad -k \frac{\partial T}{\partial n} = h_{tc} \cdot (T_{surface} - T_{mould}) \quad \text{inside the mould} \quad (12c)$$

$$4. \quad -k \frac{\partial T}{\partial n} = h_{tc} \cdot (T_{surface} - T_{amb}) + \sigma \cdot \varepsilon \cdot (T_{surface}^4 - T_{amb}^4) \quad \text{within the secondary and tertiary zones} \quad (12d)$$

$$5. \quad -k \frac{\partial T}{\partial n} = \dot{q} \quad \text{beneath the rollers} \quad (12e)$$

The boundary conditions are divided into the area of the mould, the area of the secondary cooling and the area of the tertiary cooling.

The initial condition for the investigation is the setting of the temperature in the individual points of the mesh. A suitable temperature is the highest possible temperature, i.e. the pouring temperature. The explicit difference method is used for solving this problem. The property of this method is that the stability of the calculation is dependent on the magnitude of the time step. The model has incorporated a method for the

adaptation of the time step, i.e. the time step entered by the operator is merely a recommendation and the software modifies it throughout the calculation [4].

The heat transfer coefficient along the entire caster

The cooling by the water nozzles has the main influence and it is therefore necessary to devote much attention to establish the relevant heat-transfer coefficient of the forced convection. Commercially sold models of the temperature field describe the heat-transfer coefficient beneath the nozzles as a function of the incident quantity of water per unit area. They are based on various empirical relationships. This procedure is undesirable. The model discussed in this paper obtains its heat-transfer coefficients from measurements of the spraying characteristics of all nozzles used by the caster on a so-called hot plate in an experimental laboratory [6, 7] and for a sufficient range of operational pressures of water and a sufficient range of casting speeds of the blank (i.e. casting speed). This approach represents a unique combination of experimental measurement in a laboratory and a numerical model for the calculation of the non-linear boundary conditions beneath the cooling nozzle.

Figure 5 presents the measured values of the heat transfer coefficients processed by the temperature model software. For nozzle configuration, there is a graph of the 3D graph of the heat transfer coefficient beneath the nozzle. These graphs are plotted for a surface temperature of 1000 °C.

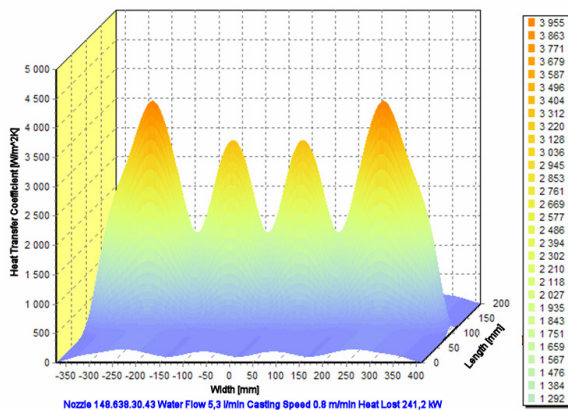


Figure 5: The heat transfer coefficient for the 148.638.30.43 nozzle – 4 nozzles in a row

The resultant heat transfer coefficient is determined by adding up the partial coefficients. This basically entails the total heat transfer coefficient because even radiation, with the introduction of the “reduced heat transfer coefficient from radiation”, was converted to convection. On these areas of the blank, where natural

convection and radiation occur, the total coefficient is given by the sum of this reduced coefficient from the radiation and the coefficient of the actual natural convection. In the area beneath the nozzle, the resultant heat transfer coefficient is obtained as the sum of the forced convection coefficient gained from the laboratory temperature measurement and the reduced heat transfer coefficient from radiation [2].

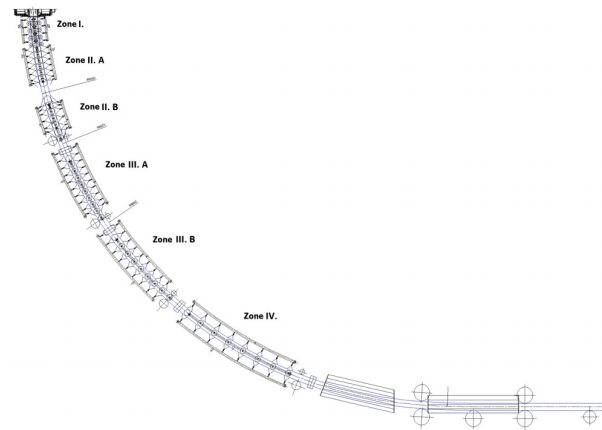


Figure 6: Positions of the nozzles along the billet caster in 6 individual zones

On a specific caster, the nozzles of the secondary cooling are divided into several independent regulation zones, which enables the formation of the temperature field of the blank. Figure 6 shows the 6 individual regulation zones and Figure 7 shows the courses of the resultant heat transfer coefficients along the small radius of the billet caster. Figure 8 shows the 13 individual regulation zones and Figure 9 shows the courses of the resultant heat transfer coefficients along the small radius of the slab caster.

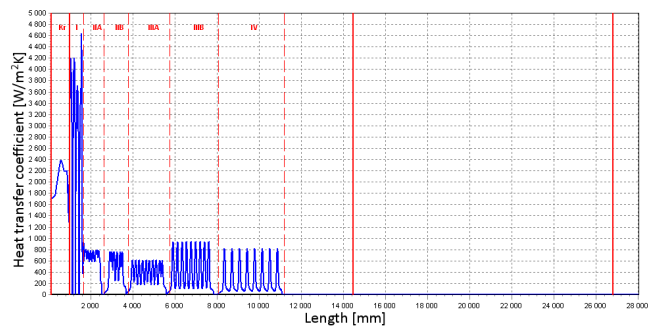


Figure 7: The resultant heat transfer coefficient along the small radius of the billet caster

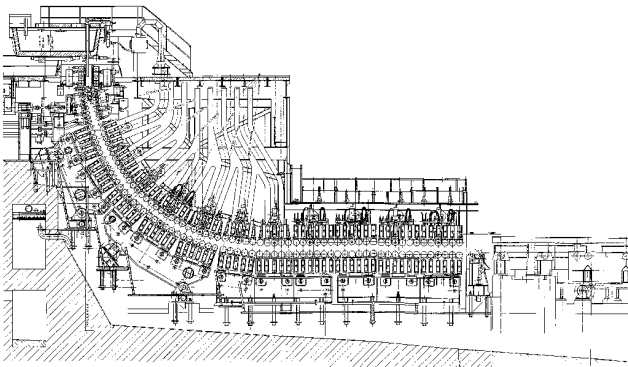


Figure 8: Positions of the nozzles along the slab caster in 13 individual zones

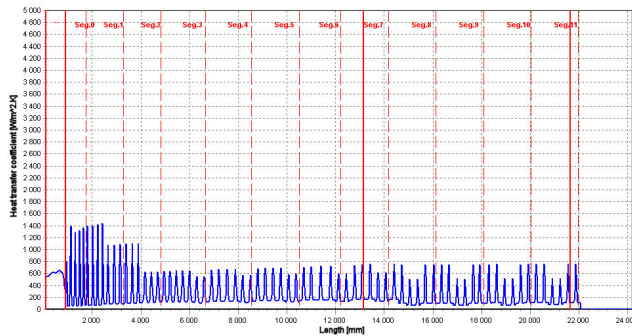


Figure 9: The resultant heat transfer coefficient along the small radius of the slab caster

Transient analysis

Figure 10 and 11 show the output from a simulation of a failure in the secondary cooling (e.g. of the pumps in circuits 8 and 9 of slab caster) using the dynamic model on the analysis of the functioning of the secondary cooling. If there had really been such a failure, the temperature model would have warned the operator in time for him/her to decide what action to take.

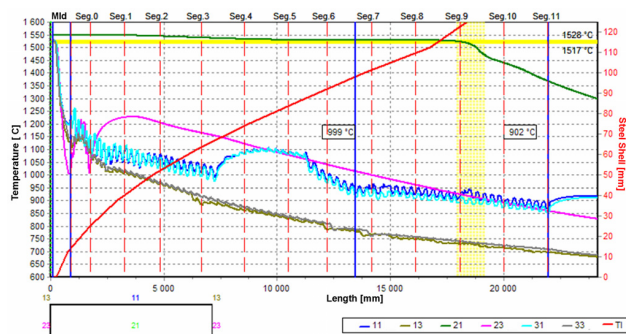


Figure 10: Calculation results from the simulated failure in the secondary cooling in circuits 8 and 9 of slab caster

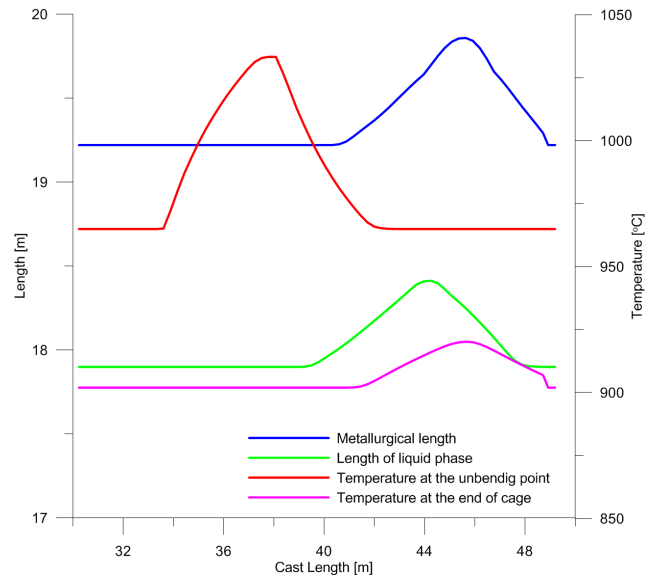


Figure 11: The history of the selected quantities during the simulated failure in the secondary cooling in circuits 8 and 9

Most quantities of the caster, from the first and second control levels (including the surface temperatures measured by pyrometers), are entered into the software of the temperature model where they are appended by a number of calculated quantities and successively stored into the database of the application server. The operator can choose from these measured and calculated quantities and plot them in the form of trends. Since there are many quantities, only the main ones have been chosen in order to include more influences.

For this purpose, a graph was plotted in order to show the casting speed, the superheat temperature, the metallurgical length and the surface temperatures calculated by the model and measured using pyrometers in the same places. When comparing the measured temperatures with the calculated, the calculated temperature is the average temperature of four points of the mesh that are the closest to the pyrometers.

Furthermore, it is necessary to monitor the heat released through the mould via individual plates and the surface temperatures beneath the mould.

Figure 12 illustrates a testing case of a step change in the casting speed from 0.8 to 0.5 m/min and back. Such step decreases in speed can be caused by an intervention of the breakout system. The return to the original speed in reality happens more slowly and it is the dynamic model that makes it possible to find the optimal method for controlling the speed and secondary cooling.

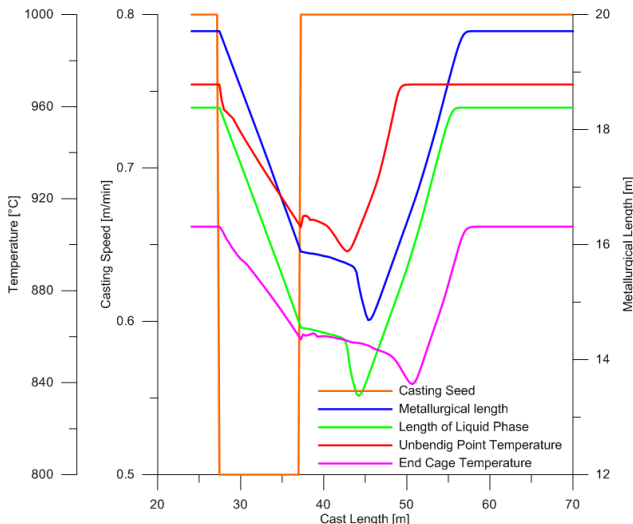


Figure 12: A simulated change in speed and the response of the calculated quantities

Figure 13 shows an example of real data from the dynamic model of a 1530×180 mm slab upon the intervention of the breakout system. This intervention brought about a drop in the casting speed from 1.22 to 0.5 m/min and an increase back to the original value. It is interesting to observe the course of the measured temperatures in the unbending point and at the end of the cage where the drop in the casting speed is visible. It is quite obvious that the calculated temperature history will facilitate any decision-making by the operator regarding the control of the caster.

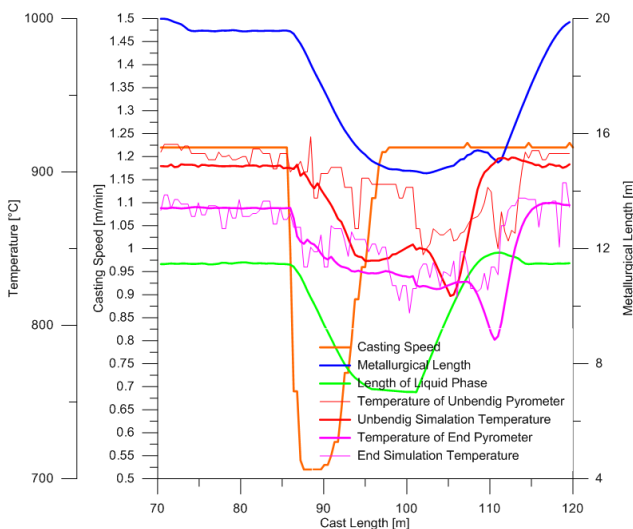


Figure 13: An example of the drop in the casting speed upon the intervention of the breakout system

Figure 14 shows the quantities from a real melt and the data from the dynamic model. Towards the end of the casting process, there is an increase in the casting

speed as a result of a reduction in the superheating temperature.

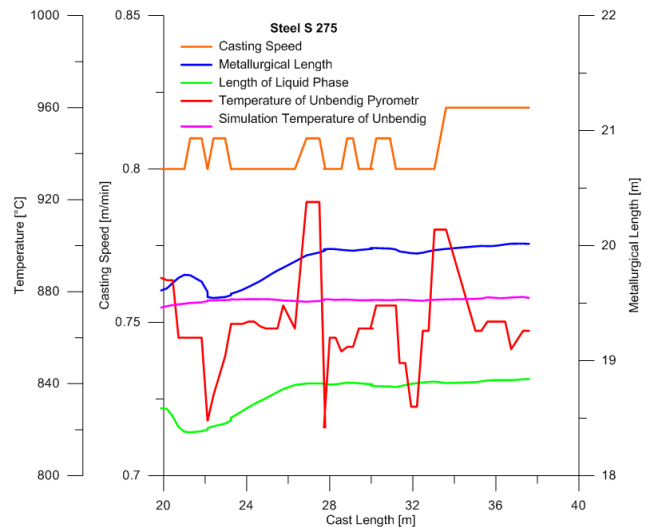


Figure 14: The history of the selected quantities

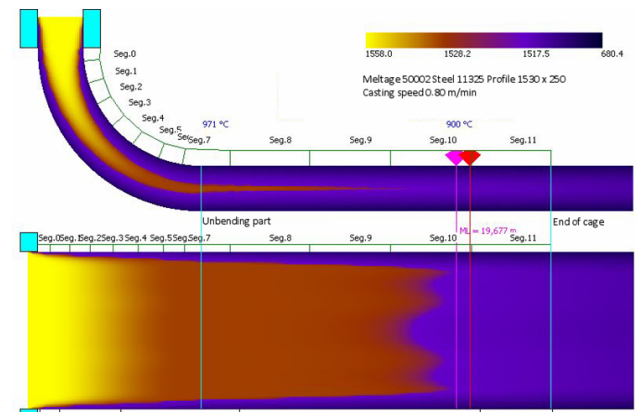


Figure 15: Temperature field of the S 275 class steel slab

Figure 15 presents the calculated temperature field for casting parameters: the casting speed 0.8 m/min, the superheating temperature 30 °C and the profile of the slab 1530×250 mm, just like the flow of water through the secondary-cooling zone.

On-line model of the temperature field

A temperature model can be considered as successfully implemented if it is integrated into the existing information and control systems of a caster. Figure 16 illustrates a specific case of integration of models into the casting technology control system of a caster for the casting of steel and the quality system for slab casting at EVRAZ VITKOVICE STEEL. The caster control room is equipped with a two-processor workstation where the on-line dynamic model is running nonstop and which

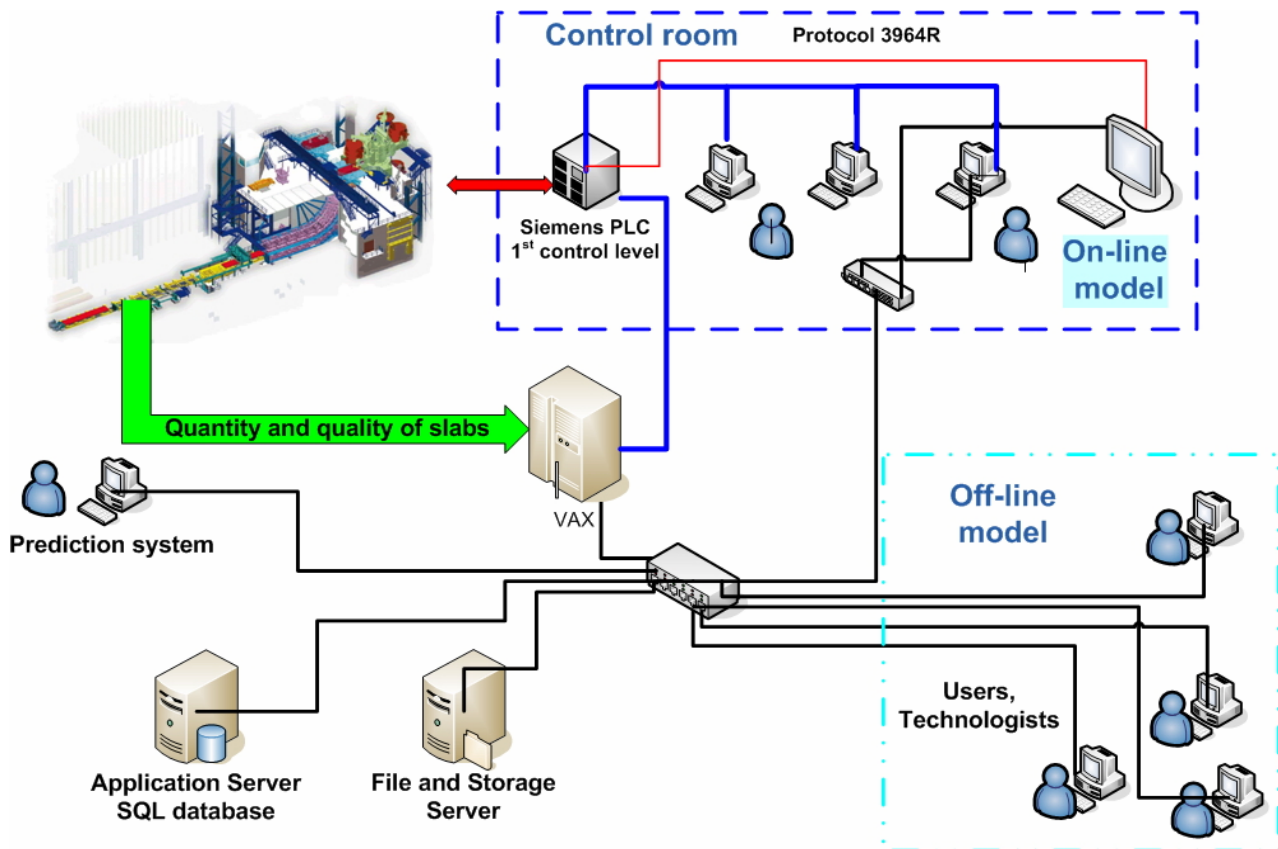


Figure 16: The casting technology control system

receives data from the 1st and 2nd levels of control via an interface program. The input data are verified, the erroneous data being filtered out and the temperature field calculated. On the computer monitor, the operator can select from the various forms of output. According to the results, the on-line model makes recommendations for the operator in order to facilitate the control of the concasting process. The computer is simultaneously a web server and therefore the technologists and other users of the steelworks web can observe all of the data coming from the on-line temperature model. The results from the calculated temperature field of the concasting of each melt are stored on an archive server for a period of six months. All filtered input data and their relevant aggregated quantities pertaining to the temperature field are stored into the database of an application server, where they are re-calculated for a specific slab and linked to the information on the quality of the slab and, successively, on the quality of the sheet steel produced from this slab. The data from the application server are then passed on to the prediction system.

The users (i.e. technologists) can record the real-time data from the on-line model into their off-line model of the temperature field, carry out any necessary changes

in the input parameters (e.g. to alter the secondary cooling or the casting speed). After simulation on the off-line model, it is possible to determine how the temperature field changes after carrying out these changes. Another application of the off-line version is in the occurrence of defects on/in the actual slab or sheet steel. The user can read the temperature field from the archive server using the dynamic model and – using the off-line model – analyse any likely causes of defects and prepare the necessary measures for the defects never to occur again. The off-line model will (in future) enable the reading of quantities and their dependences from the application server and, using statistical methods and the relationships among these quantities and defects, will look for the cause in the original temperature field of the concasting from a specific melt. However this will be the task of the mathematical-stochastic prediction model.

Based on these rules and parametric studies, it is possible to split the problem of the control of the casting parameters into two separate parts:

- The control of the casting speed according to the superheating temperature and the actual (calculated) metallurgical length.

- The control of the water flow according to the required surface temperatures, where the courses of the cooling curves are used. The set of cooling curves was proposed and optimized using the off-line model.

The dynamic model does not control the water flow in the individual circuits directly, but only recommends that the operator switches to another cooling curve. Here, the model is tuned according to the measured surface temperatures with the aid of pyrometers in two places of the caster. Both pyrometers measure the upper surface of the billet. The first pyrometer is positioned very close to the unbending point. Originally, it served as a reference for checking the function of the secondary cooling. The value given by this pyrometer now serves for the comparison of the temperatures calculated by the model with the actually measured ones. The measured temperature must be higher than the prescribed (i.e. a concasting which is too cold must not be unbent). On the other hand, the temperatures measured upon the output from the cage by the second pyrometer should be lower than those prescribed in the technological procedure.

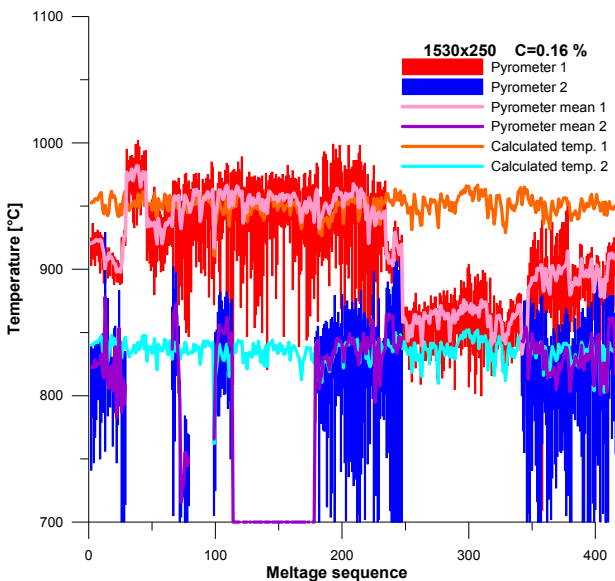


Figure 17: A comparison of the measured and calculated temperatures of a 1530×250 mm slab

Figure 17 compares the average values of the measured surface temperatures in two points with the average calculated temperatures in the same points. The graphs indicate that the measured and calculated values are practically identical in terms of their trends. Comparing the absolute values, it is possible to see that there are long intervals where the deviation is significant and, on the other hand, there are intervals where the values are identical. Furthermore, there are

sequences of melts where one pyrometer is out of operation. The conclusion here is that the calculated values of the temperatures are much more reliable and give values that are much more suitable for the prediction system or the secondary-cooling regulation. Another reason why there can be a difference between the measured and calculated temperatures is the state of the secondary cooling.

Figure 18 compares the average values of the measured surface temperatures in the same points. Comparing the absolute values, it is possible to see that there are long intervals where the deviation is significant and, on the other hand, there are intervals where the values are identical.

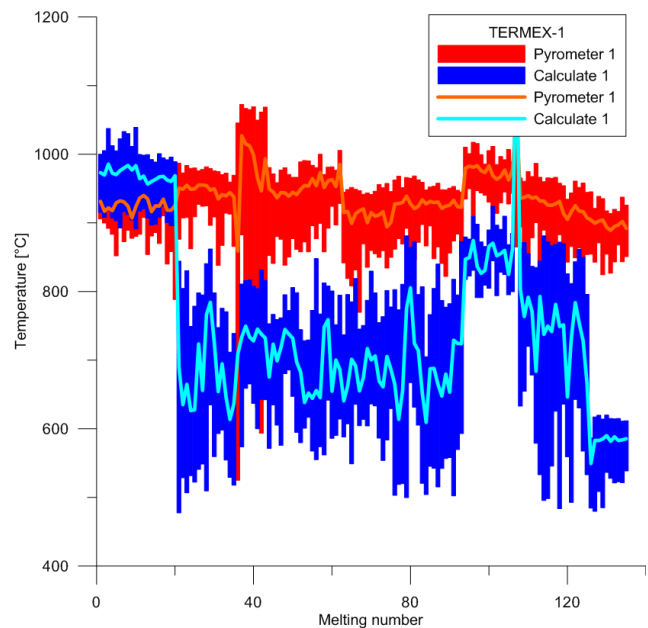


Figure 18: The measured and calculated temperatures of billet

Conclusion

This paper introduces a 3D numerical model of the temperature field (for concasting of steel) in the form of in-house software. The model includes the main thermodynamic transfer phenomena during the solidification of concasting. The temperature model is used for monitoring and for parametric studies of the changes in the chemical composition, the casting speed, the superheating temperature and the dimensions of the concast slab. The paper has introduced the dynamization of the mathematical model of the temperature field of a slab in its off-line and especially on-line versions, which have been incorporated into the operations and systems of casters at EVRAZ VITKOVICE STEEL and TRINECKE ZELEZARNY. This proves the usefulness of the model for real applications, but also the reliability and robustness of the used

numerical methods and other software. The model has been applied in the calculation and setting of the constants of the caster control system, the simulation of the caster operation even under non-standard situations (e.g. failures of parts of the secondary cooling in the unexpected slowing down of casting), planned maintenance of the machine or its structural improvements, the utilization of information that helps the operator to make spontaneous changes in the control of the machine and in the utilization of monitoring and control of quality, the direct control of the casting speed and the flow of water in the individual zones of the secondary cooling of the prediction system.

Nomenclature

A	area	[m ²]
c	specific heat capacity	[J/kg.K]
htc	heat transfer coefficient	[W/m ² .K]
H_v	volume enthalpy	[J/m ³]
k	heat conductivity	[W/m.K]
L_{LIQ}	length of the liquid phase	[m]
L_{MET}	metallurgical length	[m]
q	specific heat flow	[W/m ²]
QX, QY, QZ	heat flows	[W]
Q_{source}	heat source	[W/m ³]
T	temperature	[K]
T_{mould}	temperature of mould wall	[K]
T_{amb}	ambient temperature	[K]
$T_{surface}$	surface temperature	[K]
T_{cast}	melt temperature	[°C]
$T_{unbending}$	temperature in unbending part	[°C]
T_{end}	temperature in end of cage	[°C]
x, y, z	axes in given direction	[m]
V_x, V_y, V_z	casting speed in given direction	[m/s]
VX, VY, VZ	heat conductivity	[W/K]
ρ	density	[kg/m ³]
σ	Stefan-Boltzmann constant	[W/m ² .K ⁴]
ε	emissivity	[-]
τ	time	[s]

Acknowledgments

This analysis was conducted using a program devised within the framework of the project GA CR No. 106/08/0606, 106/09/0940.

References

- [1] Brimacombe, J. K.: The Challenge of Quality in Continuous Casting Process. *Metallurgical and Materials Trans*, B, Volume 30B, (1999) P. 553-566.
- [2] Miettinen, J.; Louhenkilpi; Laine, J.: Solidification analysis package IDS. Proceeding of General COST 512 Workshop on Modelling in Materials Science and Processing, M. Rappaz and M. Kedro eds., ECSC-EC-EAEC, Brussels, Luxembourg, (1996).

- [3] Richard, A.; Harding, Kai Liu; Beckermann, Ch.: A transient simulation and dynamic spray cooling control model for continuous steel casting, *Metallurgical and materials transactions*, volume 34B, (2003) P.297-302.
- [4] Kavička, F.; Stetina, J.; Sekanina, B.; Stransky, K.; Dobrovska, J.; Heger, J. The optimization of a concasting technology by two numerical models. *Journal of Materials Processing Technology*. 2007. 185(1-3). P.152
- [5] Thomas, B. G.; O'Malley, R. J.; Stone, D. T.: Measurement of temperature, solidification, and microstructure in a continuous cast thin slab. Paper presented at Modeling of Casting, Welding and Advanced Solidification Processes VIII, San Diego, CA, TMS (1998).
- [6] Pihoda, M., Molinek, J., Pyszko, R., Velicka, M., Vaculik, M. Burda, J.: Heat Transfer during Cooling of Hot Surfaces by Water Nozzles. *Metallurgija= Metallurgy*, vol. 48, (4), 2009, P. 235-238.
- [7] Horsky, J.; Raudensky, M.: Measurement of Heat transfer Characteristics of Secondary Cooling in Continuous Casting. In *Metal 2005*. Ostrava: TANGER, 2006. P.1-8.